of variables subject to the cuts of Eq. (3). In order to calculate the reflection of process (B) on the histograms relevant to process (A) and vice versa, it is necessary to include information about the angular distribution in each vertex c.m. system. In all cases this was approximated by the on-shell angular distribution.[24] The π-proton angular distributions were calculated from the CERN phase-shift analysis[25] and the $\pi\pi$ angular distributions reconstructed from the phase-shift analysis of Malamud and Schlein[26] (the results are insensitive to the choice of solution) for $m<1$ GeV and for $m>1$ GeV from Wolf.[12] The DP correction at the π^-p vertices are identical to those used by Colton *et al.*[27] in an analysis of $pp \to (p\pi^-)(p\pi^+)$, in which it was demonstrated that these corrections are unnecessary for $M \geq 1.6$ GeV.

[24] Colton *et al.* (Ref. 27) have shown in a series of papers on pp studies that this is a rather good approximation for peripherally produced π-proton systems. See also E. Colton and P. Schlein, in *Proceedings of the Conference on $\pi\pi$ and $K\pi$ Interactions* (Argonne National Laboratory, Argonne, Ill., 1969), p. 1.

[25] A. Donnachie, R. G. Kirsopp, and C. Lovelace, CERN Report No. CERN-TH 838, Addendum, 1967 (unpublished).

[26] See Ref. 16.

[27] E. Colton, P. E. Schlein, E. Gellert, and G. A. Smith, Phys. Rev. D **3**, 1063 (1971).

PHYSICAL REVIEW D VOLUME 3, NUMBER 9 1 MAY 1971

Pole Extrapolation of the Reactions $\pi^-p \to \pi^-\pi^+n$ and $\pi^+p \to \pi^+\pi^-\Delta^{++}(1238)$*

EUGENE COLTON
Lawrence Radiation Laboratory, University of California, Berkeley, California 94720

AND

ERNEST MALAMUD
National Accelerator Laboratory, Batavia, Illinois 60510

(Received 21 December 1970)

Experimental differential cross sections from data on the reactions $\pi^-p \to \pi^-\pi^+n$ and $\pi^+p \to \pi^+\pi^-\Delta^{++}(1238)$ have been extrapolated to the one-pion-exchange pole to obtain the $\pi^+\pi^-$ elastic scattering cross section from threshold to 1.4 GeV. Consistent results are obtained in three c.m. energy ranges for both reactions. The data have been fitted to several t-dependent extrapolation functions, and the results of the fits are tabulated and plotted as a function of $\pi^+\pi^-$ effective mass. In particular, we find cross sections of approximately 25 and 125 mb, respectively, at the K and central $\rho^0(765)$ mass positions.

I. INTRODUCTION

THE proper extraction of $X\pi$ elastic scattering cross sections from data on the reactions $Xp \to X\pi^+n$ and $Xp \to X\pi^-\Delta^{++}(1238)$ [for $X=\pi$, K, p] has been the goal of many experiments since the work of Goebel[1] and Chew and Low.[1] Many analyses, which include the fits of experimental differential cross sections to various theoretical formulas as well as numerous extrapolation procedures, have either assumed or attempted to show that single-pion exchange is dominant in the above reactions in the intermediate energy region. More recently, however, Kane[2] has pointed out that other exchanges (e.g., ρ, A_2) are just as, if not more, important in the region of small momentum transfer. Thus it appears that if pion exchange is indeed present in a reaction, an appropriate extrapolation procedure must be carried out in order to isolate and determine its magnitude.

In this paper we present a determination of the $\pi^+\pi^-$ elastic scattering cross section by means of a modified Chew-Low[1] extrapolation to the pion-exchange pole in the reactions

$$\pi^-p \to (\pi^-\pi^+)n \tag{1a}$$

and

$$\pi^+p \to (\pi^+\pi^-)\Delta^{++}(1238). \tag{1b}$$

Pole-extrapolation analyses[3,4] of reaction (1a) which yield similar results have been performed previously. This analysis, however, reports the first high-statistics pole extrapolation of reaction (1b) using data at different beam energies. We show below that our results from reactions (1a) and (1b) are consistent with each other and with earlier determinations,[3,4] thus supporting the one-pion-exchange (OPE) assumption and the validity of our pole-extrapolation procedure.

We assume (for small momentum transfer) that the processes depicted in Figs. 1(a) and 1(b) play significant roles in reactions (1a) and 1(b), respectively. The extrapolation procedure which we use has been shown[5] to successfully yield π^+p elastic scattering cross sections in the region of the $\Delta^{++}(1238)$ resonance from peripheral data on the reaction $pp \to (p\pi^+)n$ at 6.6 GeV/c incident laboratory beam momentum. The method in-

* Supported in part by the U. S. Atomic Energy Commission.

[1] C. Goebel, Phys. Rev. Letters **1**, 337 (1958); G. F. Chew and F. E. Low, Phys. Rev. **113**, 1640 (1959).

[2] G. L. Kane, in *Experimental Meson Spectroscopy 1970*, edited by C. Baltay and A. H. Rosenfeld (Columbia U. P., New York, 1971), p. 1.

[3] S. Marateck *et al.*, Phys. Rev. Letters **21**, 1613 (1968).

[4] J. P. Baton *et al.*, Phys. Letters **33B**, 525 (1970).

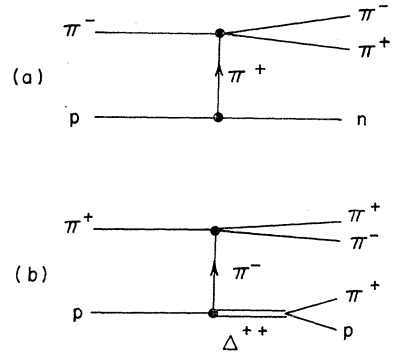

FIG. 1. Single-pion-exchange diagrams for the reactions considered in this paper.

volves first normalizing the experimental differential cross section $(d\sigma/dt)_{\text{expt}}$ at $\pi^+\pi^-$ effective mass m, to a function which behaves similarly with t, but which reduces to the required value at the pion-exchange pole. The normalized data points are then fitted to a low-order polynomial in t. The pole value of the polynomial with best-fit parameters yields the $\pi^+\pi^-$ elastic scattering cross section. The procedure does not require extrapolation of quantities with poles and does not require the pion-exchange cross section to vanish at zero momentum transfer in the data of reaction (1a). Effects such as absorption and Reggeization of the exchanged pion are thus allowed for.

In Sec. II we list and examine the data used in the extrapolation. The extrapolation procedure and the fits to the data are discussed in Secs. III and IV, respectively. The results and conclusions are put forth in Sec. V.

II. EXPERIMENTAL DATA

The analysis of the data[6] of reaction (1a) has been performed upon a total of 20 541 events which have been subdivided into 5082, 7728, and 7731 events corresponding to intervals in center of mass energy of 2.0–2.37, 2.37–2.49, and 2.49–2.70 GeV, respectively. The analysis of the data[7] for reaction (1b) has been performed upon a total of 17 729 events of the type

$$\pi^+p \to \pi^+\pi^-\pi^+p, \tag{2}$$

which are subdivided into 7207, 4653, and 5869 events corresponding to three intervals in c.m. energy. The first two intervals occupy ranges of 2.57–2.78 and 2.78–2.98 GeV in c.m. energy and the third interval contains events with nominal beam momenta of 6.94 (3.73 GeV c.m.) and 8.4 (4.08 GeV c.m.) GeV/c. For the purpose of further discussion we denote the separation of events into c.m. energy intervals as experiments, characterized by the ordinal numbers 1, 2, and 3. The

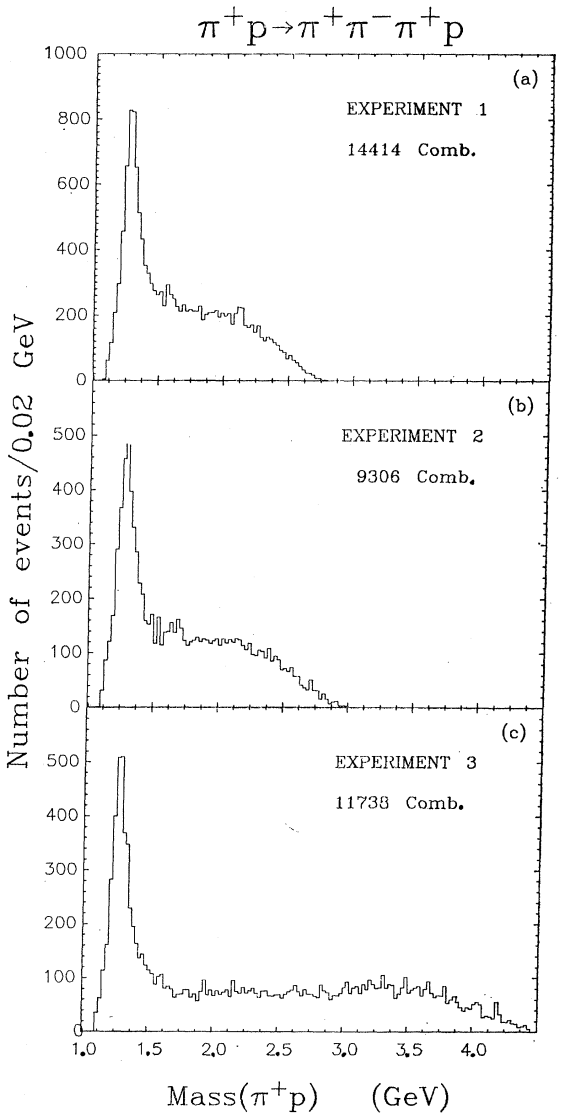

FIG. 2. π^+p effective-mass spectra for the reaction $\pi^+p \to \pi^+\pi^-\pi^+p$. Two combinations are plotted for each event.

[5] Z. Ming Ma *et al.*, Phys. Rev. Letters **23**, 342 (1969). For additional description of the pole-extrapolation procedure see, e.g., E. Colton and P. E. Schlein, in *Proceedings of the Conference on $\pi\pi$ and $K\pi$ Interactions* (Argonne National Laboratory, Argonne, Ill., 1969), p. 1.

[6] The following laboratories and collaborations have generously contributed their data on the reaction $\pi^-p \to \pi^-\pi^+n$: Pennsylvania-Saclay-Orsay-Bari-Bologna [V. Hagopian *et al.*, Phys. Rev. **145**, 1128 (1966); Y. Pan. *ibid.* **152**, 1183 (1966)]; Purdue [D. H. Miller *et al.*, *ibid.* **153**, 1423 (1967)]; Lawrence Radiation Laboratory [L. Jacobs, LRL Report No. UCRL-16877, 1966 (unpublished)]; Argonne-Toronto-Wisconsin [D. R. Clear *et al.*, Nuovo Cimento **49A**, 399 (1967); A. W. Key *et al.*, Phys. Rev. **166**, 1430 (1968)].

[7] The following laboratories and collaborations have generously contributed their data on the reaction $\pi^+p \to \pi^+\pi^-\pi^+p$. Rochester-Yale [P. Slattery, H. Kraybill, B. Forman, and T. Ferbel, Nuovo Cimento **50A**, 377 (1967)]; Lawrence Radiation Laboratory [D. Brown *et al.*, Phys. Rev. Letters **19**, 664 (1969); D. Brown *et al.*, Phys. Rev. D **1**, 3053 (1970)]; Lawrence Radiation Laboratory [G. Goldhaber *et al.*, Phys. Rev. Letters **12**, 336 (1964)]; University of California, San Diego [Maris Abolins *et al.*, Phys. Rev. Letters **11**, 381 (1963)]; Columbia-Rutgers [M. Rabin, R. Plano, C. Baltay, P. Franzini, L. Kirsch, H. Kung, and N. Yeh, Bull. Am. Phys. Soc. **12**, 9 (1967)].

events used in this analysis represent a portion of the data used in the phase-shift analysis of Malamud and Schlein.[8] Some of the $\pi^-\pi^+n$ events have also been utilized in the pole-extrapolation and phase-shift analyses of Marateck *et al.*[3]

The strong $\Delta^{++}(1238)$ component in reaction (2) can be seen in the histograms of π^+p effective mass in Figs. 2(a)–2(c) (corresponding to the three experiments). Two combinations are plotted for each event. In order to obtain events corresponding to reaction (1b), we require

$$1.12<M<1.34 \text{ GeV}, \tag{3}$$

where M is the π^+p effective mass. If both M combinations for an event fall within the cut (3), then we use

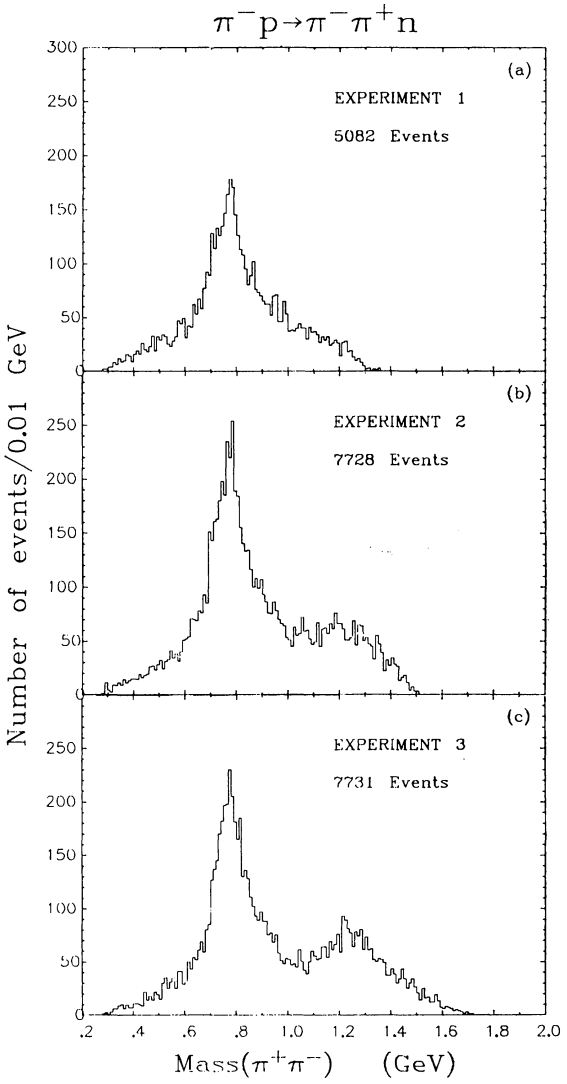

FIG. 3. $\pi^+\pi^-$ effective-mass spectra for the reaction $\pi^-p\to\pi^+\pi^-n$.

[8] E. Malamud and P. E. Schlein, in *Proceedings of the Conference on $\pi\pi$ and $K\pi$ Interactions* (Argonne National Laboratory, Argonne, Ill., 1969), p. 93.

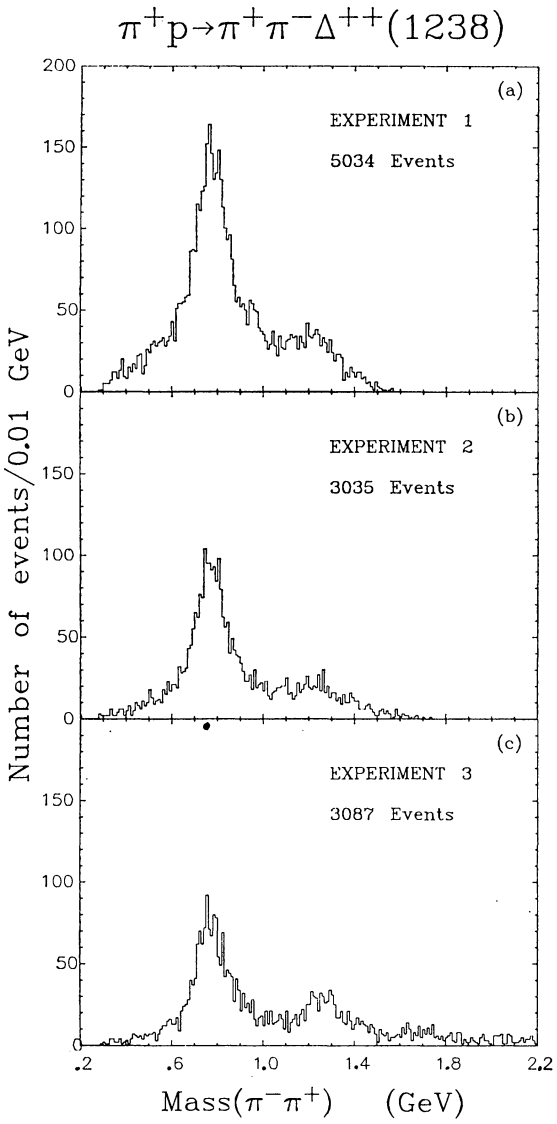

FIG. 4. $\pi^+\pi^-$ effective-mass spectra for events of the type $\pi^+p\to\pi^+\pi^-(\pi^+p)$, where $1.12<M(\pi^+p)<1.34$ GeV. If both π^+p combinations fall within these limits, we use that combination with the smallest t from the target proton to the π^+p system. One $\pi^+\pi^-$ combination is plotted for each event.

that combination with the smaller value of t measured from the target proton to that outgoing $\Delta^{++}(1238)$ combination. The four-momentum-transfer squared (t) is chosen to be positive in the physical region. The $\pi^+\pi^-$ effective-mass spectra for reactions (1a) and (1b) are presented in Figs. 3 and 4, respectively. The presence of $\rho^0(765)$ production is obvious. Additional structure near 1250 MeV for the higher c.m. energy experiments is evidence for $f^0(1260)$ resonance production.

III. EXTRAPOLATION PROCEDURE

The experimental $d\sigma/dt$ for reactions (1a) and (1b) have been extrapolated to the OPE pole for different

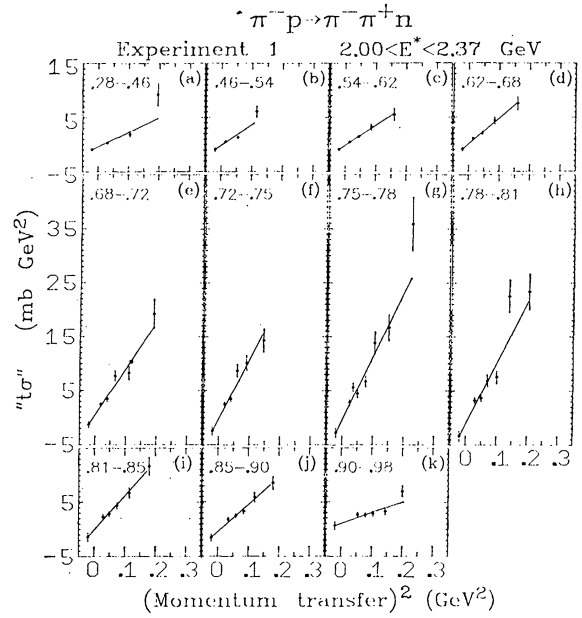

FIG. 5. Experimental "$t\sigma$" quantities for reaction (1a) and experiment 1, defined in Eq. (7a), for the 11 denoted $\pi^+\pi^-$ mass regions. Straight lines and the extrapolated points at $t=-\mu^2$ represent the expansion "$t\sigma$"$=a+bt$ using for a and b the best-fit values obtained in the least-squares fits.

$\pi^+\pi^-$ mass regions (for each experiment) following the procedure of Ma *et al.*[5] This procedure differs from the traditional Chew-Low method in that the experimental differential cross section $(d\sigma/dt)_{\text{expt}}$ is normalized to the pole equation modified by a suitable form factor, instead of to the pole equation alone. For reactions (1a) and (1b), we write[9]

$$\frac{d^2\sigma}{dtdm}=\frac{1}{4\pi m_p{}^2P_L{}^2}\frac{g^2}{4\pi}\frac{t}{(t+\mu^2)^2}[m^2q(m)\sigma(m)]F(m,t) \quad (4a)$$

and

$$\frac{d^3\sigma}{dtdmdM}=\frac{1}{4\pi^3m_p{}^2P_L{}^2}\frac{[m^2q(m)\sigma(m)]}{(\hbar c)^2}\times\frac{[M^2Q(M)\sigma(M)]}{(t+\mu^2)^2}F(m,M,t), \quad (4b)$$

respectively. In Eqs. (4), μ (m_p) are the pion (proton) rest masses, P_L is the laboratory beam momentum, $g^2/4\pi=29.2$, m (M) are the $\pi^+\pi^-$ (π^+p) effective masses, $q(Q)$ are the momenta in the $\pi^+\pi^-$ (π^+p) rest systems, and the σ functions are the on-mass-shell vertex elastic scattering cross sections. All quantities have the units GeV or mb, except F which is dimensionless.

The form factors (F) used in Eqs. (4) can be any smooth continuous functions which reduce to unity at the pion-exchange pole. To obtain suitable F functions, we first multiply the phenomenological Dürr-Pilkuhn (DP)[10] $\rho^0(765)$ vertex factor by the t-dependent form factor[11] which Wolf[12] found was necessary in order to describe the t distributions of various quasi-two-body processes. Defining a function G, we write

$$G(m,t)=\left(\frac{2.3-\mu^2}{2.3+t}\right)^2\left(\frac{q_t}{q}\right)^2\left[\frac{1+(8.3q)^2}{1+(8.3q_t)^2}\right], \quad (5)$$

where q_t is the momentum of the incoming beam pion evaluated in the $\pi^+\pi^-$ rest system. The form factor

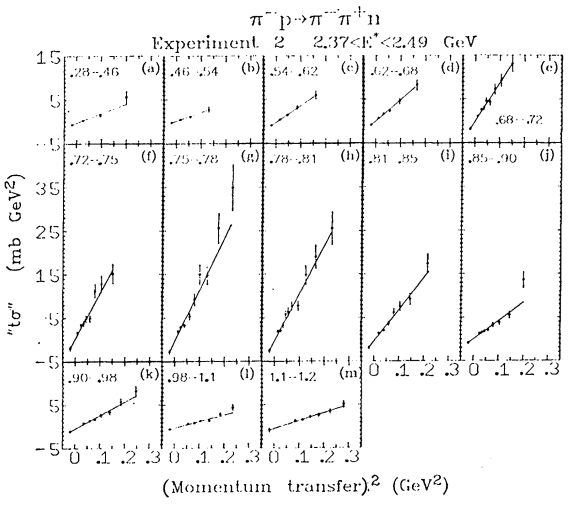

FIG. 6. Experimental "$t\sigma$" quantities for reaction (1a) and experiment 2, defined in Eq. (7a), for the 13 denoted $\pi^+\pi^-$ mass regions. Straight lines and the extrapolated points at $t=-\mu^2$ represent the expansion "$t\sigma$"$=a+bt$ using for a and b the best-fit values obtained in the least-squares fits.

[9] See, e.g., E. Ferrari and F. Selleri, Nuovo Cimento Suppl. 24, 453 (1962).

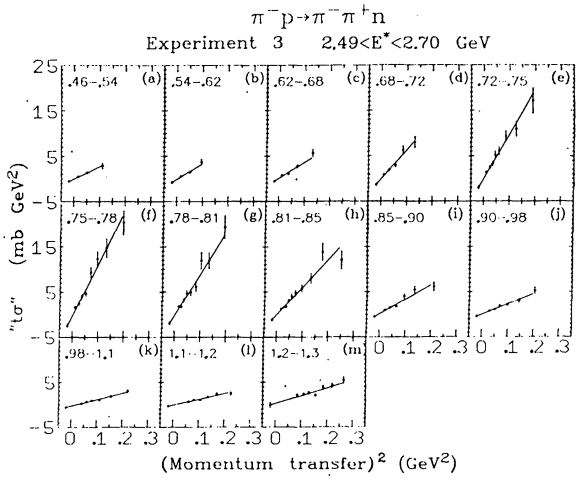

FIG. 7. Experimental "$t\sigma$" quantities for reaction (1a) and experiment 3, defined in Eq. (7a), for the 13 denoted $\pi^+\pi^-$ mass regions. Straight lines and the extrapolated points at $t=-\mu^2$ represent the expansion "$t\sigma$"$=a+bt$ using for a and b the best-fit values obtained in the least-squares fits.

[10] H. P. Dürr and H. Pilkuhn, Nuovo Cimento 40, 899 (1965)
[11] G. Goldhaber *et al.* Phys. Letters 6, 62 (1963).
[12] G. Wolf, Phys. Rev. Letters 19, 925 (1967).

TABLE I. Results of fits of the "$t\sigma$" data points, for experiment 1 in $\pi^- p \to (\pi^-\pi^+)n$, to the assumed forms $a+bt$, bt, and $bt+ct^2$.

$\pi^+\pi^-$ mass range (GeV)	Events	"$t\sigma$"$=a+bt$ σ (mb)	"$t\sigma$"$=a+bt$ a/μ^2 (mb)	"$t\sigma$"$=a+bt$ Prob. (%)	"$t\sigma$"$=bt$ σ (mb)	"$t\sigma$"$=bt$ Prob. (%)	"$t\sigma$"$=bt+ct^2$ σ (mb)	"$t\sigma$"$=bt+ct^2$ $c\mu^2$ (mb)	"$t\sigma$"$=bt+ct^2$ Prob. (%)
0.28–0.46	56	47±13	−20±8	2	14±2	<1	3±4	3±1	22
0.46–0.54	70	48±19	−9±12	2	33±4	4	15±10	5±3	8
0.54–0.62	104	46±12	−9±8	92	32±3	65	27±6	1±1	68
0.62–0.68	159	46±18	2±13	94	49±4	99	49±8	0±1	93
0.68–0.72	261	64±31	22±22	13	95±6	15	100±13	−1±2	8
0.72–0.75	225	122±44	−11±31	11	107±7	18	107±17	0±3	11
0.75–0.78	297	140±47	−21±35	1	112±7	2	86±15	5±2	5
0.78–0.81	267	167±50	−55±38	1	96±6	1	70±13	5±2	4
0.81–0.85	215	70±39	−7±31	96	61±4	92	56±11	1±2	89
0.85–0.90	200	77±37	−26±30	82	44±3	78	36±9	1±1	88
0.90–0.98	209	−34±38	53±32	13	29±2	7	34±7	−1±1	4

TABLE II. Results of fits of the "$t\sigma$" data points, for experiment 2 in $\pi^- p \to (\pi^-\pi^+)n$, to the assumed forms $a+bt$, bt, and $bt+ct^2$.

$\pi^+\pi^-$ mass range (GeV)	Events	"$t\sigma$"$=a+bt$ σ (mb)	"$t\sigma$"$=a+bt$ a/μ^2 (mb)	"$t\sigma$"$=a+bt$ Prob. (%)	"$t\sigma$"$=bt$ σ (mb)	"$t\sigma$"$=bt$ Prob. (%)	"$t\sigma$"$=bt+ct^2$ σ (mb)	"$t\sigma$"$=bt+ct^2$ $c\mu^2$ (mb)	"$t\sigma$"$=bt+ct^2$ Prob. (%)
0.28–0.46	53	35±11	−14±7	20	14±2	6	6±4	2±1	80
0.46–0.54	65	12±11	7±7	65	24±3	52	28±7	−1±1	36
0.54–0.62	139	47±10	−9±6	72	32±3	33	25±5	2±1	66
0.62–0.68	226	46±12	3±7	88	50±3	94	50±7	0±1	85
0.68–0.72	300	95±19	−7±12	78	85±5	83	81±11	1±2	76
0.72–0.75	331	103±26	5±18	23	110±6	31	111±14	0±3	22
0.75–0.78	418	144±26	−24±18	2	110±6	2	80±11	6±2	28
0.78–0.81	418	128±26	−18±18	37	104±5	37	95±10	2±2	38
0.81–0.85	370	97±21	−23±15	42	65±3	28	54±7	2±1	52
0.85–0.90	323	46±18	−3±14	10	41±2	16	33±6	2±1	23
0.90–0.98	343	55±13	−24±10	71	24±1	20	17±3	1±0	95
0.98–1.1	252	30±12	−16±10	8	12±1	7	7±2	1±0	26
1.1 –1.2	251	40±25	−22±22	88	15±1	82	11±3	0±0	96

TABLE III. Results of fits of the "$t\sigma$" data points, for experiment 3 in $\pi^- p \to (\pi^-\pi^+)n$, to the assumed forms $a+bt$, bt, and $bt+ct^2$.

$\pi^+\pi^-$ mass range (GeV)	Events	"$t\sigma$"$=a+bt$ σ (mb)	"$t\sigma$"$=a+bt$ a/μ^2 (mb)	"$t\sigma$"$=a+bt$ Prob. (%)	"$t\sigma$"$=bt$ σ (mb)	"$t\sigma$"$=bt$ Prob. (%)	"$t\sigma$"$=bt+ct^2$ σ (mb)	"$t\sigma$"$=bt+ct^2$ $c\mu^2$ (mb)	"$t\sigma$"$=bt+ct^2$ Prob. (%)
0.46–0.54	66	30±13	−2±8	89	26±3	95	25±7	0±2	80
0.54–0.62	110	41±13	−6±8	26	31±3	40	22±8	3±2	50
0.62–0.68	173	28±12	7±8	5	40±3	8	36±7	1±2	3
0.68–0.72	212	70±17	−5±11	68	62±4	78	57±10	1±2	72
0.72–0.75	320	101±21	−2±13	81	98±6	90	103±11	−1±2	86
0.75–0.78	415	121±23	−6±15	60	112±6	67	111±11	0±2	58
0.78–0.81	368	96±23	−3±15	27	92±5	37	84±10	2±2	35
0.81–0.85	405	55±15	5±11	35	63±3	42	67±6	−1±1	39
0.85–0.90	300	22±13	10±9	13	35±2	15	38±4	0±1	10
0.90–0.98	332	21±10	2±8	62	23±1	75	23±3	0±0	62
0.98–1.1	277	27±6	−13±5	43	11±1	7	7±2	1±0	31
1.1 –1.2	258	15±13	−3±12	42	12±1	55	12±2	0±0	42
1.2 –1.3	333	4±32	13±28	9	19±1	14	18±4	0±0	8

appearing in Eq. (4a) is given by

$$F(m,t)=\left[\frac{1+7.1(q_n)^2}{1+7.1(q_n)_t^2}\right]G(m,t), \qquad (6a)$$

where $(q_n)_t^2$ is the momentum squared of the incoming target proton evaluated in the neutron rest system, and $(q_n)^2$ is this quantity taken on-shell. Similarly the form factor appearing in Eq. (4b) is given by the product of the phenomenological DP $\Delta^{++}(1238)$ vertex factor and $G(m,t)$:

$$F(m,M,t)=\left(\frac{Q_t}{Q}\right)^2\left[\frac{1+(4Q)^2}{1+(4Q_t)^2}\right]\times\left[\frac{(M+m_p)^2+t}{(M+m_p)^2-\mu^2}\right]G(m,t), \qquad (6b)$$

where Q_t is the momentum of the incoming target proton evaluated in the Δ^{++} rest system. The use of

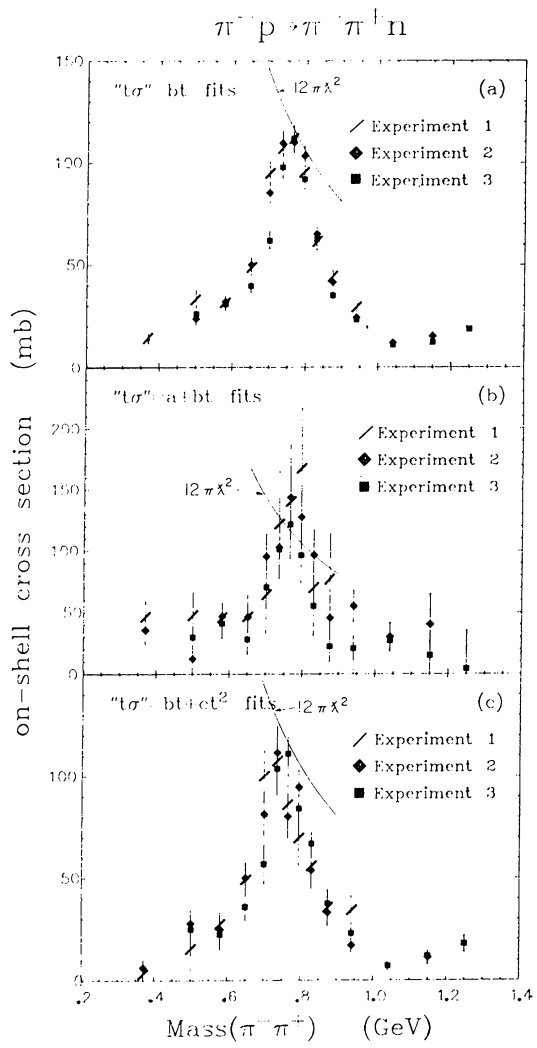

FIG. 8. Extrapolated on-mass-shell $\pi^+\pi^-$ elastic scattering cross sections, obtained in least-squares fits of the "$t\sigma$" points shown in Figs. 5–7 to the assumed forms bt, $a+bt$, and $bt+ct^2$, plotted as a function of $\pi^+\pi^-$ effective mass. Curves are $12\pi\lambda^2$ which is the unitarity limit for an elastic p-wave $\pi\pi$ resonance.

form factors such as (6a) and (6b) along with other appropriate DP factors have been shown[12,13] to describe experimental Chew-Low distributions for strong-interaction reactions of the classes $Xp \to X\pi^+n$ and $Xp \to X\pi^-\Delta^{++}$ (for $X=\pi$, K, p) over a large range of beam momenta. The usefulness of this procedure lies in the fact that the complexity of the t dependence of the function to be extrapolated is minimized, thereby decreasing the order of the polynomial which is fitted to the experimental points.

The functions which we extrapolate to the pole for each specified interval in $\pi^+\pi^-$ mass (Δm) are

[13] P. Schlein, in *Proceedings of the Conference on $\pi\pi$ and $K\pi$ Interactions* (Argonne National Laboratory, Argonne, Ill., 1969), pp. 1 and 446; see also review talk by P. Schlein, in *Meson Spectroscopy*, edited by C. Baltay and A. H. Rosenfeld (Benjamin, New York, 1968), p. 161.

$$\text{"}t\sigma\text{"} = \frac{(d\sigma/dt)_{\text{expt}}}{(1/t)(d\sigma/dt)_{\text{DP-OPE}}} \tag{7a}$$

for reaction (1a) and

$$\text{"}\sigma\text{"} = \frac{(d\sigma/dt)_{\text{expt}}}{(d\sigma/dt)_{\text{DP-OPE}}} \tag{7b}$$

for reaction (1b). The expressions $(d\sigma/dt)_{\text{DP-OPE}}$ in Eqs. (7a) and (7b) are Eqs. (4a) and (4b), respectively, after integration over the variable(s) other than t. The on-shell cross sections $\sigma(m)$ are set equal to 1 mb in calculating the denominator so that at the pole $-\mu^2\sigma^{\pi^+\pi^-}{}_{\text{on-shell}} = \text{"}t\sigma\text{"}$ and $\sigma^{\pi^+\pi^-}{}_{\text{on-shell}} = \text{"}\sigma\text{"}$ for reactions (1a) and (1b), respectively. Polynomials in t are then fitted to the experimental "$t\sigma$" and "σ" points. Note that if $(d\sigma/dt)_{\text{DP-OPE}}$ has precisely the same t dependence as $(d\sigma/dt)_{\text{expt}}$ than "$t\sigma$" points can be described by the form bt and "σ" points are independent of t. Thus the need for other terms in the polynomial expressions allows for departure of $(d\sigma/dt)_{\text{DP-OPE}}$ from $(d\sigma/dt)_{\text{expt}}$.

IV. FITS TO DATA

The experimental "$t\sigma$" values for reaction (1a), calculated[14] using Eq. (7a), are displayed in Figs. 5–7. The three figures are subdivided into 11, 13, and 13

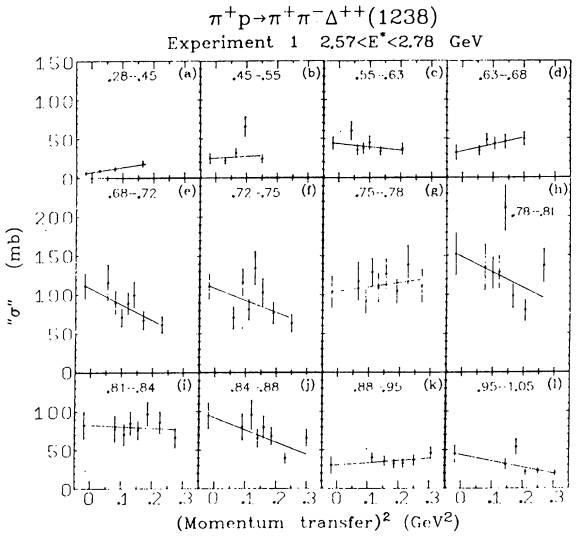

FIG. 9. Experimental "σ" quantities for reaction (1b) and experiment 1, defined in Eq. (7b), for the 12 denoted $\pi^+\pi^-$ mass regions. Straight lines and the extrapolated cross sections at $t=-\mu^2$ represent the expansion "σ"$=a+bt$ using for a and b the best-fit values obtained in the least-squares fits.

[14] We use the expression

$$\text{"}t\sigma\text{"} = \frac{c}{\int dl\,dm} \sum_{i=1}^{N} \left[\frac{t}{(d^2\sigma/dl\,dm)_{\text{DP-OPE}}} \right]_i$$

to evaluate "$t\sigma$" for a given $\Delta t\Delta m$ bin. Here c is the mb/event factor, the sum is over the events in the sample, and the bracketed quantity is evaluated for each event. The integral $\int dl\,dm$ is over that portion of the $\Delta t\Delta m$ bin in question which is included in the physical region of the Chew-Low plot.

TABLE IV. Results of fits of the "σ" data points, for experiment 1 in $\pi^+p \to (\pi^+\pi^-)\Delta^{++}(1238)$, to the assumed forms a and $a+bt$.

$\pi^+\pi^-$ mass range (GeV)	Events	"σ"$=a$ σ (mb)	Prob. (%)	"σ"$=a+bt$ σ (mb)	$b\mu^2$ (mb)	Prob. (%)
0.28–0.45	61	11±1	16	6±3	1±1	86
0.45–0.55	98	27±3	1	25±7	0±1	<1
0.55–0.63	159	38±3	50	44±8	−1±1	45
0.63–0.68	152	43±4	60	32±10	2±1	71
0.68–0.72	237	78±5	17	112±17	−4±2	50
0.72–0.75	233	84±6	3	111±17	−3±2	5
0.75–0.78	288	113±7	70	104±21	1±3	62
0.78–0.81	258	115±7	<1	152±27	−4±3	<1
0.81–0.84	217	79±5	77	83±18	0±2	69
0.84–0.88	209	60±4	1	95±17	−3±1	5
0.88–0.95	194	37±3	74	30±11	1±1	65
0.95–1.05	139	23±2	3	45±12	−2±1	7

parts, corresponding to the denoted regions of $\pi^+\pi^-$ effective mass, respectively. Least-squares fits of the data in Figs. 5–7 have been performed separately to the forms $a+bt$, bt, and $bt+ct^2$. The resulting confidence levels and the best-fit values of the parameters, as well as the extrapolated on-mass-shell $\pi^+\pi^-$ elastic scattering cross sections are presented in Tables I–III. The numbers listed in column 2 of the tables represent only the peripheral (small-t) events used to calculate the experimental "$t\sigma$" points. All of the fits listed in the tables have acceptable confidence levels ($\geq 1\%$) except for the "$t\sigma$"$=bt$ fit in the lowest $\pi^+\pi^-$ mass range in Table I. Therefore, the experimental differential cross

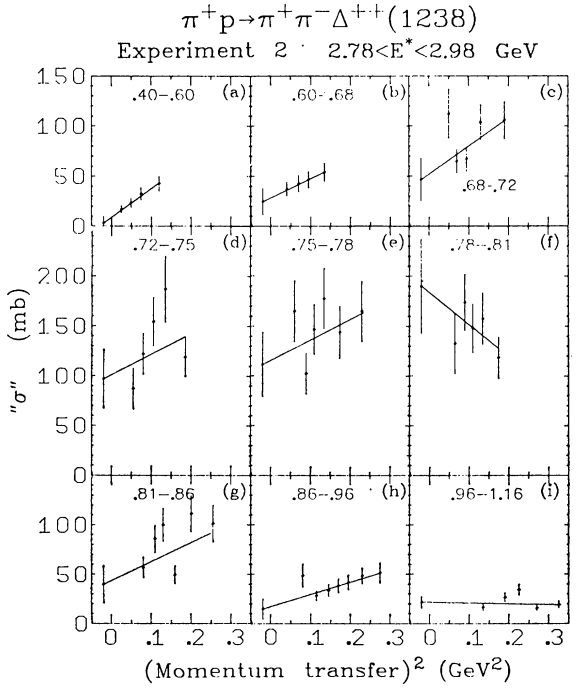

FIG. 10. Experimental "σ" quantities for reaction (1b) and experiment 2, defined in Eq. (7b), for the 9 denoted $\pi^+\pi^-$ mass regions. Straight lines and the extrapolated cross sections at $t=-\mu^2$ represent the expansion "σ"$=a+bt$ using for a and b the best-fit values obtained in the least-squares fits.

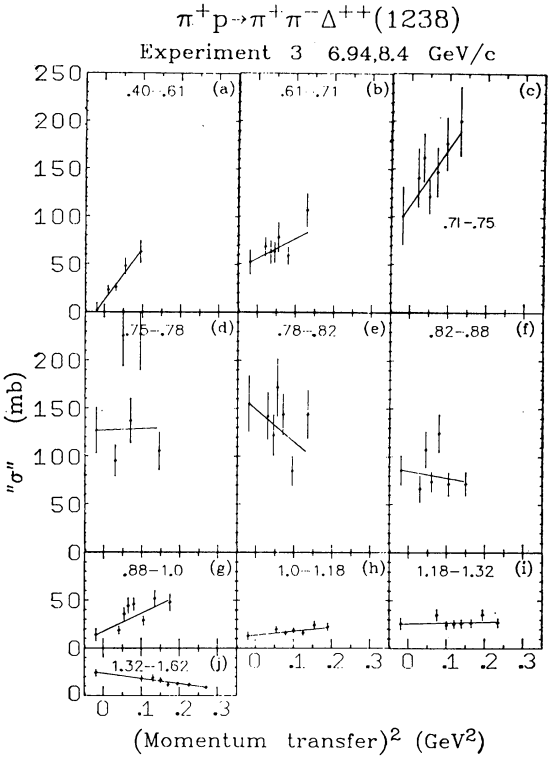

FIG. 11. Experimental "σ" quantities for reaction (1b) and experiment 3, defined in Eq. (7b), for the 10 denoted $\pi^+\pi^-$ mass regions. Straight lines and the extrapolated cross sections at $t=-\mu^2$ represent the expansion "σ"$=a+bt$ using for a and b the best-fit values obtained in the least-squares fits.

sections $(d\sigma/dt)_{\text{expt}}$ appear to be adequately represented by $(d\sigma/dt)_{\text{DP-OPE}}$ in the t and m ranges considered here. The straight lines and the extrapolated points at $t=-\mu^2$ (in Figs. 5–7) represent the expansion "$t\sigma$" $=a+bt$ using for a and b the best-fit values obtained in the least-squares fits. Tables I–III indicate that the a and c parameters obtained in the fits are generally consistent with zero. However, they are negative and positive, respectively, in the central ρ mass region. Thus, the resulting extrapolated cross sections from the $a+bt$ and $bt+ct^2$ fits are larger and smaller than the bt fit value, respectively, in the central ρ-mass region. The

TABLE V. Results of fits of the "σ" data points, for experiment 2 in $\pi^+p \to (\pi^+\pi^-)\Delta^{++}(1238)$, to the assumed forms a and $a+bt$.

$\pi^+\pi^-$ mass range (GeV)	Events	"σ"$=a$ σ (mb)	Prob. (%)	"σ"$=a+bt$ σ (mb)	$b\mu^2$ (mb)	Prob. (%)
0.40–0.60	110	24±3	1	3±7	6±2	95
0.60–0.68	120	44±4	50	25±14	4±3	99
0.68–0.72	147	81±7	9	47±22	5±3	15
0.72–0.75	160	125±10	8	97±30	4±4	6
0.75–0.78	182	143±11	28	112±33	4±4	25
0.78–0.81	163	143±11	55	190±47	−6±6	58
0.81–0.86	198	71±5	<1	40±19	4±2	<1
0.86–0.96	201	38±3	20	15±11	2±1	62
0.96–1.16	163	20±2	1.5	22±6	0±0	<1

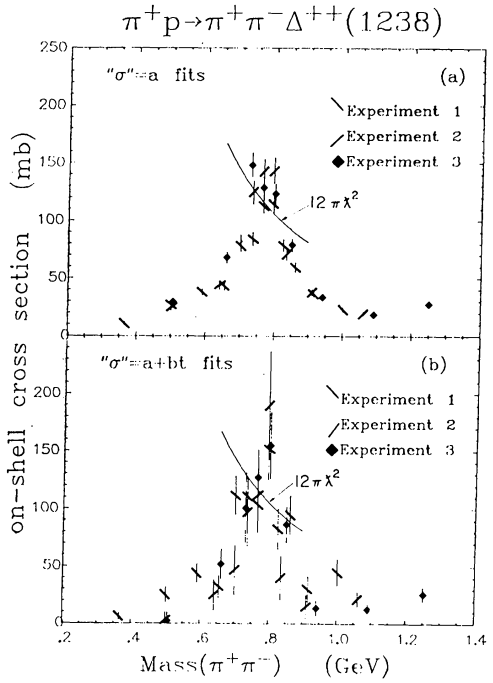

FIG. 12. Extrapolated on-mass-shell $\pi^+\pi^-$ elastic scattering cross sections, obtained in least-squares fits of the "σ" points shown in Figs. 9–11 to the assumed forms a and $a+bt$, plotted as a function of $\pi^+\pi^-$ effective mass. Curves are $12\pi\lambda^2$, which is the unitarity limit for an elastic p-wave $\pi\pi$ resonance.

extrapolated cross sections listed in Tables I–III are plotted in Figs. 8(a)–8(c) as a function of $\pi^+\pi^-$ effective mass. The smooth curves drawn in Fig. 8 are $12\pi\lambda^2$, which represent the unitarity limit for an elastic p-wave $\pi\pi$ resonance. The points in Figs. 8(a)–(8c) occur below, above, and below the unitarity limit at the ρ-mass peak, respectively.

The experimental "σ" points for reaction (1b), calculated[15] using Eq. (7b), are displayed in Figs. 9–11. These three figures are subdivided into 12, 9, and 10 parts, corresponding to the denoted regions of $\pi^+\pi^-$ effective mass, respectively. Least-squares fits of the data in Figs. 9–11 have been performed separately to the assumed forms a and $a+bt$. The resulting confidence levels and the best-fit values of the parameters, as well as the extrapolated on-mass-shell $\pi^+\pi^-$ elastic scattering cross sections, are presented in Tables IV–VI. As above, the numbers listed in column 2 of each table represent only the peripheral events used to calculate the experimental "σ" points. Five of the "σ"$=a$ fits listed in Tables IV–VI have unacceptable confidence levels ($<1\%$). In the remaining cases, however, the experimental differential cross sections $(d\sigma/dt)_{\text{expt}}$ appear to be adequately described by $(d\sigma/dt)_{\text{DP-OPE}}$ in the t and m ranges considered. The straight lines and the extrapolated cross sections at $t=-\mu^2$ (in Figs. 9–11) represent the expansion "σ"$=a+bt$ using for a and b the best-fit values obtained in the least-squares fits. Figures 9–11 indicate an abrupt change in slope parameter b while passing through the ρ region. The change from positive to negative values of b accounts for the large values of extrapolated cross section observed in the $\pi^+\pi^-$ mass bin starting at 0.78 GeV. The extrapolated cross sections listed in Tables IV–VI are displayed in Figs. 12(a) and 12(b) as a function of $\pi^+\pi^-$ effective mass. The smooth curves drawn in Fig. 12, again represent the p-wave unitarity limit. The points in both Figs. 12(a) and (12(b) exceed the unitarity limit at the ρ-mass peak.

[15] We use the expression

$$\text{"}\sigma\text{"}=\frac{c}{\int dtdmdM}\sum_{i=1}^{N}\left[\frac{1}{(d^3\sigma/dtdmdM)_{\text{DP-OPE}}}\right]_i$$

to evaluate "σ" for a given $\Delta t\Delta m\Delta M$ bin. The other quantities are defined in Ref. 14.

V. DISCUSSION AND CONCLUSIONS

The extrapolated $\pi^+\pi^-$ elastic scattering cross sections resulting from the different fits appear to be similar for the three experiments in all cases. This observation supports the OPE hypothesis and indicates that the systematic effects induced by errors in the experimentally determined cross sections for reactions (1a) and (1b) are small compared to the statistical errors. In Table VII we list the extrapolated cross sections, averaged over the three experiments, from both reactions (1a) and (1b). These cross sections are also plotted in Figs. 13(a) and 13(b), respectively, as a function of $\pi^+\pi^-$ mass. The cross sections obtained from each of the assumed forms for "$t\sigma$" and "σ" appear to be quantitatively consistent everywhere except in the central ρ-mass region. In particular, a value of roughly 25 mb is observed at the K mass. In the central ρ-mass bin the "$t\sigma$"$=a+bt$ and "σ" fits indicate an average cross section of roughly 125 mb. The "$t\sigma$"$=bt$ and "$t\sigma$"$=bt+ct^2$ fits yield cross sections which are somewhat smaller at the ρ-mass peak. The latter effect has also been observed in the earlier analysis by Marateck *et al.*[3] One expects a significant s-wave contribution[16] at 0.765 GeV so the results of our "$t\sigma$"$=a+bt$ fits are

TABLE VI. Results of fits of the "σ" data points, for experiment 3 in $\pi^+p\to(\pi^+\pi^-)\Delta^{++}(1238)$, to the assumed forms a and $a+bt$.

		"σ"$=a$		"σ"$=a+bt$		
$\pi^+\pi^-$ mass range (GeV)	Events	σ (mb)	Prob. (%)	σ (mb)	$b\mu^2$ (mb)	Prob. (%)
0.40–0.61	122	29±3	<1	2±8	11±3	52
0.61–0.71	199	68±5	26	52±13	4±3	30
0.71–0.75	210	148±10	35	101±30	12±7	55
0.75–0.78	183	129±10	<1	127±24	0±5	<1
0.78–0.82	205	123±9	6	155±29	−7±6	5
0.82–0.88	211	79±6	9	86±16	−1±3	6
0.88–1.0	231	33±2	<1	14±7	4±1	1
1.0 –1.18	215	18±1	46	13±5	1±1	52
1.18–1.32	256	27±2	62	26±6	0±1	50
1.32–1.62	218	12±1	4	25±4	−1±1	86

[16] D. Morgan and G. Shaw, Phys. Rev. D 2, 520 (1970).

TABLE VII. Extrapolated $\pi^+\pi^-$ elastic scattering cross sections, averaged over the three experiments (in mb).

	$\pi^-p \to (\pi^-\pi^+)n$				$\pi^+p \to (\pi^+\pi^-)\Delta^{++}(1238)$		
$\pi^+\pi^-$ mass range (GeV)	"$t\sigma$" $=a+bt$	"$t\sigma$" $=bt$	"$t\sigma$" $=bt+ct^2$		$\pi^+\pi^-$ mass range (GeV)	"σ" $=a$	"σ" $=a+bt$
0.28–0.46	40±8[a]	14±1[a]	5±3[a]		0.28–0.45	11±1[b]	6±3[b]
0.46–0.54	24±8	27±2	24±4		0.45–0.55	27±3[b]	25±7[b]
0.54–0.62	45±7	32±2	25±3		0.55–0.60	35±3[b]	40±7[b]
0.62–0.68	39±8	46±2	45±4		0.60–0.68	43±2	38±7
0.68–0.72	79±12	76±3	76±6		0.68–0.72	79±4[a]	88±14[a]
0.72–0.75	104±15	105±4	106±8		0.72–0.75	106±5	107±13
0.75–0.78	132±16	111±4	93±7		0.75–0.78	124±5	114±14
0.78–0.81	116±16	97±3	85±6		0.78–0.81	123±5	159±18
0.81–0.85	69±12	63±2	61±4		0.81–0.84	87±4	90±12
0.85–0.90	34±10	39±1	36±3		0.84–0.88	62±3	66±8
0.90–0.98	34±8[a]	24±1[a]	21±2[a]		0.88–0.96	36±2	19±5
0.98–1.1	28±5[a]	12±1[a]	7±1[a]		0.96–1.18	19±1[a]	17±4[a]
1.1 –1.2	20±12[a]	13±1[a]	12±2[a]		1.18–1.32	27±2[b]	26±6[b]
1.2 –1.3	4±32[b]	19±1[b]	18±4[b]		1.32–1.60	12±1[b]	25±4[b]

[a] Average of two experiments.
[b] Based on one experiment.

probably more reliable.[17] Each of the fits indicate a ρ width (full width at half-maximum) of around 150 MeV. However, the unknown resolution inherent in data compilations such as these prevents an accurate estimation. Presumably a value such as 130 MeV would be consistent with our results.

The curves appearing in Fig. 13 were calculated from the theoretical expression for σ,

$$\sigma=4\pi\lambda^2\{3\sin^2\delta_1{}^1+\tfrac{1}{9}[\sin^2\delta_0{}^2+4\sin^2\delta_0{}^0+4\cos(\delta_0{}^2-\delta_0{}^0)\times\sin\delta_0{}^2\sin\delta_0{}^0]\}, \quad (8)$$

where $\delta_L{}^T$ is the scattering phase shift for angular momentum L and isospin T, and only s- and p-wave $\pi^+\pi^-$ elastic scattering are assumed to occur. In Eq. (8), $\sin^2\delta_1{}^1$ was taken to be a resonant p-wave Breit-Wigner distribution of mass and width 0.765 and 0.125 GeV, and the values for the s-wave phase shifts $\delta_0{}^2$ and $\delta_0{}^0$ were obtained from the analyses of Colton *et al.*[18] and of Malamud and Schlein,[8] respectively. The solid and dashed curves correspond to using the "up-up" and "up-down" solutions for $\delta_0{}^0$, respectively, in Eq. (8). Both curves agree with the averaged extrapolated cross sections below the central ρ region in both Figs. 13(a) and 13(b). Above 0.8 GeV, the dashed curve appears to agree more closely with the averaged extrapolated cross sections. The data in Figs. 13(a) and 13(b) have also been compared to the predictions of Eq. (8) using for $\delta_0{}^0$ the "down-up" solutions of both Malamud and Schlein[8] and Marateck *et al.*[3] While reasonably good agreement between the data and predictions is observed in the ρ region and above, poor agreement (the predicted σ is too low) is observed below $m=0.65$ GeV.[19]

In conclusion we have performed an extrapolation to the pion-exchange pole in reactions (1a) and (1b) in three c.m. energy regions in order to determine the $\pi^+\pi^-$ elastic scattering cross section for $\pi^+\pi^-$ effective masses below 1.4 GeV. The pole extrapolation performed here differs from earlier methods[3] in that (a)

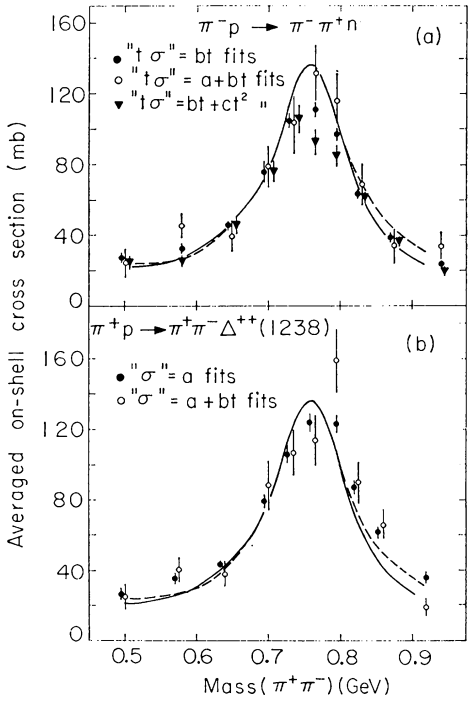

FIG. 13. Extrapolated on-mass-shell $\pi^+\pi^-$ elastic scattering cross sections, averaged over the three c.m. energy regions (or experiments). Solid and dashed curves represent the "up-up" and "up-down" solution values for $\delta_0{}^0$, respectively, in the expansion (8).

[17] Other independent work also demonstrates the presence of a nonzero component in the experimental differential cross section (e.g., "$t\sigma$") for transverse ρ production at $t=0$. The precision of this analysis is insufficient to allow us to positively verify this observation, although it does suggest a negative value. See, e.g., A. Boyarski *et al.*, Phys. Rev. Letters **20**, 300 (1968); R. Diebold and J. Poirier, *ibid.* **20**, 1552 (1968).

[18] E. Colton *et al.*, preceding paper, Phys. Rev. D **3**, 2028 (1971).

[19] We do not claim that the "up" solution is to be preferred over the "down" one below the ρ; our findings are based only upon the sets of $\delta_0{}^0$ tried in Eq. (8). More recent determinations of $\delta_0{}^0$ indicate a unique "down" solution below the ρ; in fact, these phase shifts are not too different from either the "down" or "up" solutions of Malamud and Schlein (Ref. 8) below $m=0.65$ GeV. See, e.g., J. P. Baton *et al.*, Phys. Letters **33B**, 528 (1970).

we first normalize the experimental differential cross section to the pole equation modified by appropriate form factors instead of to the pole equation alone; (b) in the analysis of the data for reaction (1a) we allow for nonvanishing contributions of the experimental differential cross section (e.g., "$t\sigma$") at $t=0$ in our fitting procedure. The results of using several t-dependent extrapolation functions to fit the data of reaction (1a) are somewhat ambiguous in that generally good fits are obtained to the "$t\sigma$" points, but the extrapolated $\pi^+\pi^-$ elastic scattering cross sections differ somewhat at the ρ-mass peak. Clearly an order-of-magnitude increase in the number of available $\pi^-p \to \pi^-\pi^+n$ events is necessary in order to accurately determine the a and c parameters in the $a+bt+ct^2$ fits to "$t\sigma$" points which are evidently required for a more precise extrapolation.

We find, additionally, that the extrapolated $\pi^+\pi^-$ elastic scattering cross sections obtained using each extrapolation function are similar for each c.m. energy region. The c.m.-energy-averaged results of reaction (1b) and the $a+bt$ fit results of reaction (1a) are consistent with each other, thus serving to verify the factorization hypothesis implicit in Eqs. (4) as well as the utility of the extrapolation procedure. Our cross-section results are also consistent with those values obtained from the plane-wave expansion for σ [Eq. (8)], which utilizes published values for the s-wave phase shifts.

ACKNOWLEDGMENT

We thank Professor Peter E. Schlein for helpful suggestions.

PHYSICAL REVIEW D VOLUME 3, NUMBER 9 1 MAY 1971

Evidence for the Internal Structure of Hadrons Obtained from Multipion Production*

J. W. ELBERT, A. R. ERWIN, AND W. D. WALKER
Physics Department, University of Wisconsin, Madison, Wisconsin 53706
(Received 28 October 1970; revised manuscript received 30 December 1970)

The striking asymmetry observed in the longitudinal momentum distribution of produced pions essentially disappears when production is viewed in a coordinate system where the incident proton has a momentum equal to $\frac{3}{2}$ that of the incident pion. Interpretation of this result in the framework of a quark model appears to suggest some simple production rules as well as several new experiments.

IN this paper we report on multipion production data from 25-GeV/c π^-p collisions in the 80-in. BNL hydrogen bubble chamber. Various general features of these data together with experimental details have been discussed in several sources previously.[1,2]

The particular feature which we would like to call attention to here can best be seen by first studying the distribution of the longitudinal momentum p_L of pions in the π^-p center-of-mass system. In Fig. 1 we have plotted the momentum component along the beam direction for each negative track from a large sample of events. Events containing strange particles with detectable decay modes have been eliminated, so that the negative charge ensures a rather pure sample of pions. There have been no kinematic constraints applied to any of the data plotted in this paper.

Two obvious features of the plot are the elastic peak at 3.5 GeV/c and the gross asymmetry of the distribution about $p_L=0$. Because it is well studied, the elastic peak has been subtracted out, leaving the dashed histogram in the figure. The asymmetry persists in the

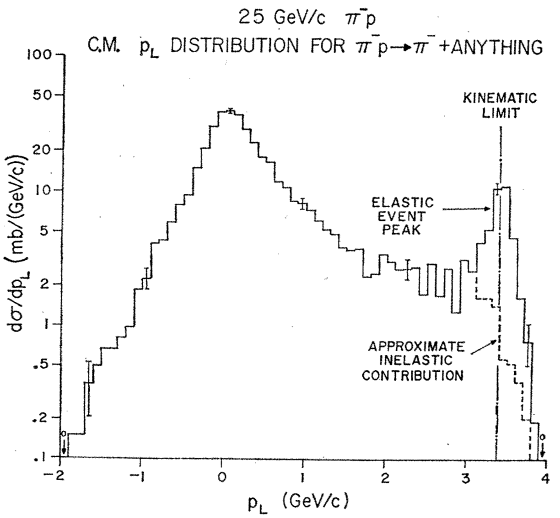

FIG. 1. Center-of-mass longitudinal momentum (c.m.s. p_L) distribution for all negative pions coming out of a π^-p collision. Subtracting out the elastic events results in the dashed histogram.

* Work supported in part by the U. S. Atomic Energy Commission under Contract Nos. AT(11-1)-881 and COO-881-289.

[1] J. W. Elbert, A. R. Erwin, S. Mikamo, D. Reeder, Y. Y. Chen, W. D. Walker, and A. Weinberg, in *Proceedings of the Topical Conference on High-Energy Collisions of Hadrons, CERN, 1968* (Scientific Information Service, Geneva, 1968), Vol. II, p. 244; Phys. Rev. Letters **20**, 124 (1968); J. W. Elbert, A. R. Erwin, W. D. Walker, and J. W. Waters, Nucl. Phys. **B19**, 85 (1970); in Proceedings of the International Conference on Expectations for Particle Reactions at the New Accelerators, University of Wisconsin, 1970 (unpublished).

[2] J. W. Waters, W. D. Walker, A. R. Erwin, and J. W. Elbert, Nucl. Phys. **B17**, 445 (1970); J. W. Waters, University of Wisconsin Ph.D. thesis (unpublished).